Implementation of a Multi-setpoint Strategy for Fire-tube Boilers Utilized in Food and Beverage Industry: Estimating the Fuel Saving Potential

Marco Tognoli, Behzad Najafi[1], Andrea Lucchini, Luigi Pietro Maria Colombo, Fabio Rinaldi

Dipartimento di Energia, Politecnico di Milano, Via Lambruschini 4, Milano 20156, Italy

Abstract

The present work aims at estimating the fuel saving potential of implementing a multi-setpoint control strategy for a fire-tube boiler that addresses a steam demand with a notable (daily) variation in the requested pressure level. The daily steam consumption profile of an Italian cheese factory is accordingly considered as the case study. Next, a dynamic PID controller is developed and tuned, aiming at enhancing the boiler's controllability at partial load conditions (in comparison with a traditional PID controller). In the next step, a multi-setpoint strategy is implemented, in which the pressure setpoint (following the desired pressure profile) is dynamically modified. The yearly fuel consumption of the boiler is then determined and is compared with the consumed fuel while employing the currently utilized constant-setpoint approach. The obtained results demonstrate that employing the proposed strategy results in reducing the yearly fuel consumption by 4.5% (cost saving of around 120000 € in 20 years of operation). The approach that is proposed in the present study can be employed by many steam end-users in the food and beverage industry, specifically in Italy, whose needed pressure level is highly variable.

Keywords: Fire-tube boiler, Dynamic modelling, Variable pressure setpoint, Fuel saving, Controllability

[1]Correspondence: behzad.najafi@polimi.it; Tel.: +39-02-2399-8518

Nomenclature

A	heat exchange surface	m^2
C^s	units conversion factor	
c_P	isobaric specific heat coefficient	$\frac{kJ}{kgK}$
c_V	isocoric specific heat coefficient	$\frac{kJ}{kgK}$
D	derivative coefficient	
$\overline{e}$	average wall tube thickness	mm
$f(x)$	inherent characteristic of the control valve	
h	specific enthalpy	kJ/kg
h_{conv}	convective heat transfer coefficient	$\frac{kW}{m^2K}$
I	integral coefficient	
k	linear conductive heat transfer coefficient	$\frac{W}{mK}$
K_{VS}	control valve flow coefficient	
L	length	m
l	water-side level height	m
LHV	fuel mass lower heating value	MJ/kg
m	mass	kg
$\dot{\overline{m}}$	hourly mass flow rate	kg/h
N	number of elements considered	
$n_{t,j}$	number of tubes in a given gas pass section at given tube banks	
P	Pressure	bar
$P_{PV(t)}$	proportional modified coefficient dependant by the process variable	
Pr	Prandtl number	

PV	process variable	
$\dot{Q}$	heat transfer rate	kW_t
R	radius	m
Re	Reynolds number	
SP	set-point variable	
T	temperature	$^\circ C$
t	time	s
T_S	simulation time	s
U	Overall heat transfer coefficient	W/m^2K
V	volume	m^3
x	valve open fraction	
Y	fuel axial heat release fraction	MJ/MJ_{tot}

Greek

η	first law efficiency term	
$\overline{\lambda}$	homogeneous latent heat of vaporization	kJ/kg
ρ	density	kg/m^3
σ	Stefan Boltzann's constant	$\frac{W}{m^2K^4}$
ε	emissivity	

Subscripts

$+$	upper side-vapor zone
$-$	lower side-liquid water zone
boiler	boiler vessel
cond	conductive
conv	convective
F	furnace
f	feedwater

$fuel$ fuel

g flue gas

H_2O water

i finite element at furnace and tubes

in inlet

$internal$ internal side

j tube bank of reference

nb nucleate-pool boiling

out outlet condition

p purge water

rad radiative

sum downstream user condition respect the steam extraction valve

t metal

v vapor

$wall$ tube wall

$water$ water side

1. Introduction

Fire-tube boilers are thermal devices, designed to generate low/medium pressure saturated steam [1], that are commonly utilized in the industrial sector. Therefore, the fuel consumption of these units has a notable impact on the thermal energy demand of many industrial activities including several processes in the food and beverage sector. Furthermore, due to the increasingly stringent environmental regulations, pollutant emissions of these boilers have received growing attention in the recent years, which should thus be considered as a critical concern in their design procedure. In this context, utilizing Stagnation Point Reverse Flow (SPRF) type combustors is an alternative solution that can be employed for reducing the NOx formation. Bobba et al. [2] investigated the production of intermediate combustion compounds in an SPRF employing a planar laser-induced fluorescent. Their results demonstrated an improved flame stability, which is attributed to the designed flue gas counter stream that causes the entrainment of exhaust gases in the flame development region. The latter phenomenon leads to a reduction in the flame temperature and enhances the presence of inert gas species due to the mixing phenomena. Both of the mentioned

effects result in a lower NOx formation in this type of furnace compared to a conventional combustion chamber. In the previous studies [3–5] that have been conducted in this area, the flame heat release rate and the kinetics were investigated through performing Large Eddy Simulations (LES) and the simulated results were later compared with the experimentally obtained data. The obtained results proved the beneficial effects of employing the SPRF combustor design on the reduction of NO_x and CO emissions. Furthermore, the authors demonstrated that, in the SPRF combustors in which the premixed combustor is utilized (as is the case in the present work), fast combustion kinetics (which commonly occurs in the area that is close to the injection port) is observed; thus, employing the SPRF configuration does not lead to an increment in the unburned fuel emissions.

Evaluating the thermal performance of these units, specifically while addressing intermittent steam demand profiles, requires the development of a detailed dynamic model. Several previous research works have been conducted on dynamic modelling of the thermal behaviour of water-tube boilers [6–14]. Previous studies, focused on conducting specific investigations on the latter units, have been dedicated to studying the water/steam side [15, 16], the water level control strategies [17, 18], and investigating the flue gas side heat transfer mechanism [19] (considering the notable effect of temperature distribution and heat flux characteristics [20]).

A limited number of investigations have been conducted on the dynamic physical modelling of fire-tube boilers for steam production. Abene et al. [21] proposed an experimentally validated physical model for a 3-pass fire-tube boiler during cold start-up and analysed the thermal-hydraulic behaviour of the system. Sorensen et al. [22] proposed a sub-model simulation approach for the estimation of the thermal performance in traditional fire-tube boilers. Similar to other power and heat generation systems [23, 24], the performance of fire-tube boilers, while meeting steam demand with an intermittent profile, can have a notable impact on the corresponding overall performance. In this context, Tognoli et al. [25] conducted a study on dynamic modelling and optimal sizing of fire-tube boilers, while addressing various demand profiles. Many studies on the dynamic thermal behaviour of fire-tube boiler have been based on Computational Fluid Dynamics (CFD) [26–29], which significantly improves the model's accuracy in terms of simulating the heat transfer mechanism and fluid motion of the flue-gas side. However, utilizing the mentioned methodology results in a notable calculation cost [30] that makes it unsuitable for investigations that require performing numerous simulations. A simplified, finite element based physical modelling approach has been proposed by Gutierrez Ortiz [31] aiming at simulating the dynamic thermal performance of fire-tube boilers for medium-pressure steam generation. The proposed detailed model facilitates obtaining an acceptable accuracy, while reducing the computational cost compared to CFD based models.

As was previously pointed out, using fire-tube boilers is a widespread solution in the industrial sector and the energy consumption of these units has a notable impact on the corresponding overall energy demand. Thus, any improvement in the thermal performance of this type of boilers and any reduction in their fuel consumption can lead to a notable energy saving and result in a significant reduction in the corresponding emissions. Several measures can be taken in order to increase the thermal performance of fire-tube boilers by

applying modifications on different design parameters. The high discharge temperature of flue gases is one of the main sources of thermal losses in these units [32]. Saidur et al. [33] has accordingly suggested that heat recovery from flue gases is an effective energy saving measure for these units and has demonstrated that the corresponding payback period is relatively low. Other studies have instead been focused on the boiler's thermal losses and the impact of local ambient conditions on the corresponding thermal performance. Bujak [34] proposed a mathematical model of the boiler's heat losses owing to the temperature difference between the unit's hot walls and the environment. The authors demonstrated that the resulting thermal losses are strongly dependant upon boiler's load, while the effect of operating pressure is less significant. Furthermore, Chao et al. [35] conducted an investigation on the effect of inlet air temperature on the boiler's thermal efficiency and determined that an increment of 10-15 $^{\circ}C$ in the inlet air temperature can enhance the boiler's efficiency by 0.8% to 1.0%.

Fire-tubes boilers utilized in industrial applications (specifically in food and beverage industry) are commonly integrated with a distribution network, which supplies the generated steam to a set of industrial appliances, each of which requires steam with a specific pressure and has a certain daily demand profile. A strategy that is commonly utilized in food and beverage firms (particularly in Italy), in order to handle the latter challenge, is to keep the pressure setpoint of the boiler constant at the maximum required pressure level. Steam pressure reducers are consequently employed in the intervals in which an appliance with a lower required pressure is fed. The mentioned strategy leads to a notable waste of energy that can clearly be evaded. An alternative strategy is to change the setpoint of the boiler based on the requirement of the appliances (instantaneous maximum needed pressure) at each interval during the day. The latter approach guarantees addressing the required supply pressure, controlled through modifying the provided fuel flow rate [36], while resulting in a notable thermal energy saving. Although extensive studies on the thermal analysis of fire-tube boilers have been conducted, no previous study has been dedicated to estimating the energy saving potential of implementing a dynamic multi-setpoint control strategy in these units or any other type of boilers.

In order to implement the multi-setpoint strategy, utilizing a promising controller that facilitates evading deviations from the desired pressure (specifically in intervals with a reduced pressure setpoint) is of notable importance. Proportional Integral Derivate (PID) controllers, motivated by their robustness and relatively simpler tuning procedure, are the most commonly utilized solutions in this area. However, their control architecture, compared to more advanced control schemes, performs in a sub-optimal manner for a range of boilers' operating conditions that are far from the scenario for which they are tuned (particularly in the presence of the system's non-linear behaviour). Chandrasekharan et al. [37] performed a comparative analysis on three commonly applied control architectures (IMC-PID, inverse decouple controller, and a Model Predictive Controller (MPC)) for a coal fired drum boiler case study. The obtained results demonstrated that the greatest deviation reduction is achieved when the system is controlled by the MPC; nevertheless, the corresponding improvement over the single-loop IMC-PID controller is marginal. An investigation on the constrained control operation during the start-up phase of a fire-tube boiler was instead conducted by

Spinelli et al. [38]. The authors investigated the critical thermal stress threshold conditions during the boiler's start-up phase and improved the utilized control strategy through implementing a non-linear MPC scheme. Nevertheless, no previous work has proposed improved control architectures for enhancing boilers' controllability while addressing dynamic steam pressure profiles and variable steam mass flow rate.

Motivated by the above-mentioned energy saving potential and the corresponding research gap, in the present work, a multi-setpoint strategy is simulated for the case study of an Italian cheese factory and the resulting reduction in the fuel consumption is determined. In this context, in order to simulate the dynamic physical behaviour of the considered fire-tube boiler (equipped with SPRF type combustor), a revised version of the model proposed by Gutiérrez Ortiz [31] is utilized . The model has been developed and experimentally calibrated and validated in a previous study conducted by the authors [39].

A dynamic PID control strategy, aiming at improving the boiler's controllability at partial load conditions, is firstly proposed and implemented. The pressure deviation (from the setpoint) that is obtained through simulating the multi-setpoint control approach, while employing the proposed dynamic PID controller, is then assessed and compared with the one achieved utilizing a conventional PID controller. Finally, the fuel consumption of the boiler while employing the proposed multi-setpoint strategy and the proposed controller is compared with the resulting fuel consumption while utilizing the conventional constant-setpoint approach. Accordingly, the key contributions of the present study are:

- Proposing and implementing a multi-setpoint steam pressure control strategy (for an industrial case study in food and beverage sector) and the assessment of the resulting fuel saving potential compared to the traditional constant pressure setpoint strategy.
- Development of a novel dynamic PID controller that facilitates reducing the pressure fluctuations and deviations (with respect to the desired pressure level in each interval), while implementing the mentioned multi-setpoint strategy (specifically during the intervals with reduced (with respect to the nominal one) pressure setpoints).

2. Mathematical model description

In the present section, the boiler's configuration and the corresponding operation principle (in the presence of the SPRF type combustor) are firstly described . Next, a detailed overview of the modelling methodology alongside the corresponding considerations and assumptions, are presented. It is noteworthy that the details of the developed model have been reported in the previous work of the authors [39] and they have been presented in the present paper in order to provide the reader with complete information.

2.1. System description

2.1.1. Description of the SPRF combustor

A Stagnation Point Reverse Flow Combustor, as schematically represented in Fig. 1, is made up of a closed cylindrical shaped tube. The pre-mixed flame develops along the main axis of the combustion chamber; flue gases are next reversed and distributed evenly at the

furnace's wall, establishing counter-current concentric streams. Therefore, the flue gases are entrained along a virtual separation layer between the inner flame development stage and the annular hot flue gas stream.

2.1.2. Boiler description

Fire-tube boilers consist of two separate regions including the flue-gas and the water-vapor sides. The combustion process is started by the burner and the flame develops in the subsequent combustion chamber. Hot flue gases then pass through the gas passes and are subsequently cooled down owing to the heat transfer occurring at the furnace and gas passes' walls (through conduction toward the water-side). Consequently, water is evaporated in the water side's vessel and the generated steam is extracted through the extraction valve. Fig. 1 provides a schematic view of the mentioned processes.

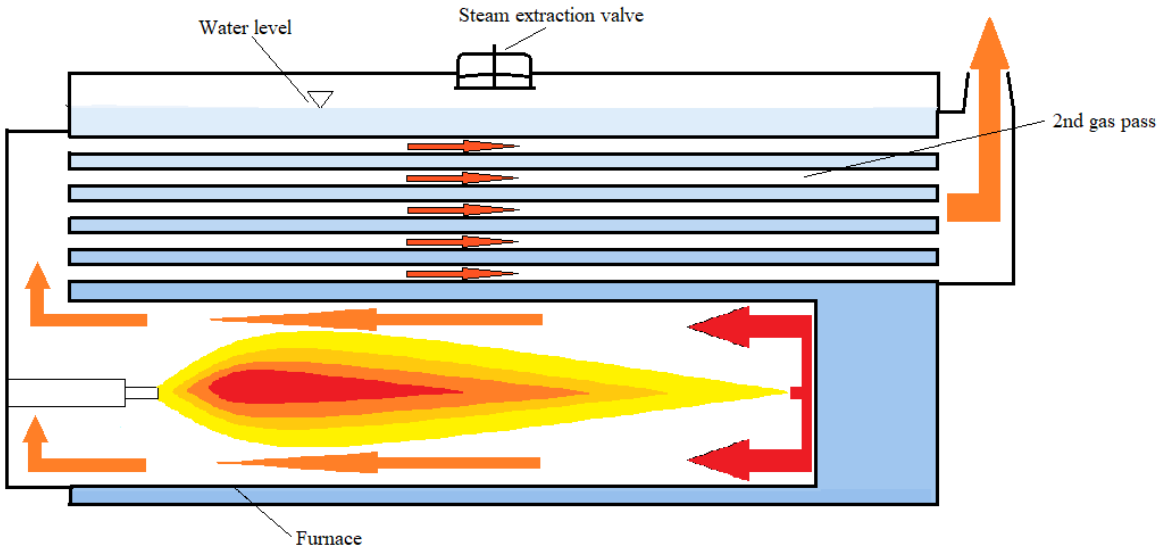

Figure 1: A simplified schematic representation of flue gas stream through a fire-tube boiler equipped with a SPRF combustor

2.2. Mathematical model

In the utilized modelling methodology, separate models for the flue-gas and water-vapor sides (employing mass, energy and momentum balances) are developed. The dynamic performance of fire-tube boilers is accordingly simulated through solving a set of partial differential equations simultaneously. It is noteworthy that utilizing the constitutive equations that describe the properties of the fluids introduces further non-linearities, which is taken into account while employing the numerical analysis. Next, an extensive validation procedure (previously presented in [39]) with experimentally obtained data is conducted. The validated model (within the tested range of operating conditions) is tuned by introducing calibration coefficients in the selected physical correlations.

2.2.1. Flue-gas side

As was previously pointed out, a sub-modelling approach is employed in the utilized modelling method. The present section describes the heat transfer mechanisms between the flue-gases and the metal walls. Combustion takes place in the first inner furnace region. The injection of natural gas and air flow is assumed to be evenly premixed within the burner modulation range. Following the previously mentioned considerations and taking into account the fact that the fluid-dynamics variations result in transient times that are much shorter than the thermal dynamic behaviour (which is the main area of interest of the present study), a few simplifications have been introduced. The combustion process is considered to be complete and the generated flue gases, for which the ideal gas behaviour is assumed, are considered to be homogeneously distributed. Considering the furnace's geometry, due to the limited D_F/L_F ratio, the axial component of radiative heat transfer mechanism is discarded. The corresponding radial component along with the convective heat transfer terms are instead calculated locally using a Finite Element Modelling (FEM) based discretization approach.

Additionally, the radiative heat transfer from the flue-gas species has not been explicitly included. Although a more detailed modelling methodology would require simulating the convective and radiative heat transfer mechanisms from the flue gases separately, considering the value of the temperature of the flue-gases at the inversion chamber (upstream of the gas passes), a marginal contribution of the net radiative heat transfer of the gray flue gases (towards the colder metal walls), compared to the dominant convective heat transfer mechanism, is expected (as reported by Beyne et al. [40]). The stream of flue gases (downstream of the inversion flow chamber) is considered to be evenly distributed between different tubes of the gas passes. The latter assumption is motivated by the fact the design approach that has been utilized by the manufacturer has resulted in similar flow paths (between the burner and the stack) through different tubes, which in turn results in the flue gas being almost evenly distributed between them. It is also noteworthy that, in order to perform multiple dynamic simulations of the boiler's behaviour, a set of simplifications should be considered in order to reduce the simulations' computational cost.

Fig. 2 schematically describes the mentioned FEM discretization approach applied to the furnace and the second gas pass axial direction. At the furnace side, the elements that have been utilized for the inner flame (forward flow) have a cylindrical shape, while those utilized for the reverse flow are hollow cylinders (co-axial with those of the forward flow), considering a virtual cylindrical separation layer at the border between the two annular counter-current flows. The mentioned modelling approach is motivated by the absence of detailed previous works dedicated to dynamic physical modelling of the thermal behaviour of SPRF type combustion chambers. The separation surface is assumed to have zero thickness with a radius equivalent to the burner's injection system. It is worth noting that Fig. 2 only shows the architecture of the utilized elements and it does not represent their shape. Considering the trade-off between the discretization error and the computational cost of the model, the optimal numbers of elements (for the furnace and gas passes separately), which guarantee mesh independence, have been identified. Accordingly, 100 elements ($N_F = 100$) have been employed for the description of the furnace side, while 20 elements have been

utilized for each gas pass ($N_j = 20$).

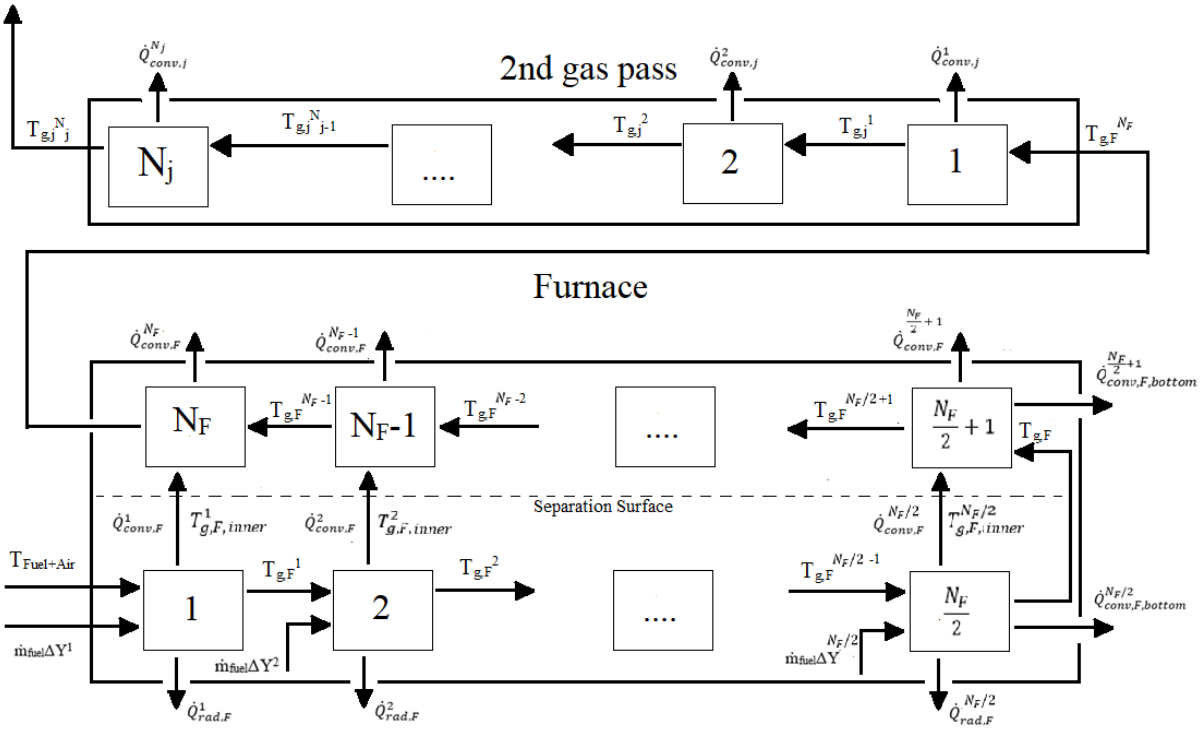

Figure 2: The employed finite element modelling architecture for the flue-gas side along furnace and second gas pass longitudinal direction

The experimental investigation conducted by Flynn et al. [41] on a boiler with a similar geometry demonstrated that considering a uniform water temperature is a reasonable assumption in the presence of saturated water and saturated vapour phases, while the heat transfer rate has to be determined. In the considered boiler, owing to the presence of nucleation promoting spots on the tube's surface and the pressurized operating condition of the boiler vessel, the nucleate pool boiling mechanism is expected. The latter assumption has been verified (as provided in the revised version of manuscript) for all the elements of tube, through determining the minimum and the maximum on-set super-heating temperature difference, employing Eq. 1 (proposed by [42]).

$$(T_{wall,j} - T_{sat}) = \frac{2\sigma_{st} T_{sat}}{r_{max} \Delta h_{lv} \rho_{water}} + \frac{\dot{q} \cdot r_{max}}{\lambda_{water}} \tag{1}$$

Considering the range of operating conditions of the considered fire-tube boiler and the maximum radius of nucleation sites of $5\mu m$ (chosen based on the tubes' characteristics), the on-set super-heating temperature difference (which represents the limiting condition to induce nucleation) is marginal compared to the surrounding saturated conditions (as reported in Table 1).

	T_{sat} [K]	$\dot{q}_{min}[kW/m^2]$	$\dot{q}_{max}[kW/m^2]$	$(\Delta T)_{onb,min}[K]$	$(\Delta T)_{onb}$
Nominal vapor pressure conditions	457.22	4.6	45.7	2.31	8.9
Reduced vapor pressure conditions	424.99	5.2	51.8	1.34	7.7

Table 1: On-set super-heating temperature difference establishing nucleation spots at nominal and partial boiler's operating conditions, and at nominal and reduced vapor pressure set-points

Considering the above mentioned assumptions and the fact that the water side heat transfer coefficient (nucleate pool boiling) is notably higher than that of the flue gas side, the wall temperature of each tube bank (separately) is considered to be homogeneously distributed.

2.2.2. Inner flame side

The heat balance equation (in dynamic terms), considering every element of the inner flame side can be formulated as in Eq. 2.

$$\frac{d}{dt} \cdot (\rho_g c_{V,g,F} V T^i_{g,F}) = \dot{m}_{fuel} LHV \Delta Y_i + \dot{m}_g \bar{c}_{P,g,F} (T^{i-1}_{g,F} - T^i_{g,F}) - \dot{q}^i_{rad,F} - \dot{q}^i_{conv,F} \tag{2}$$

Where the fractional heat release rate ΔY_i curve of a premixed burner (employed in the present investigation) is defined by the exponential function [31] represented in Eq. 3.

$$\Delta Y_i = exp\left[-4.6\left(\frac{i-1}{N_F}\right)\right] - exp\left[-4.6\left(\frac{i}{N_F}\right)\right] \tag{3}$$

Where the convective heat transfer term can be determined employing Eq. 4.

$$\dot{q}^i_{conv,F} = h^i_{conv,F,inner} \frac{2\pi R_{flame} L_F}{N_F} (T^i_{g,F} - T^i_{g,F,inner}) \tag{4}$$

No previous detailed study has been conducted on dynamic thermal modelling of the SPRF type combustor chamber and no correlation is thus available for simulating the convective heat transfer coefficient for this type of combustion chamber. Accordingly, considering the presence of turbulent flow regime in the inner-flame (forward flow) and the reverse flow, the Dittus-Boelter [43] correlation (Eq. 5) is utilized for both of these flows. It is noteworthy that (as explained in Section 4) calibration coefficients are tuned (through minimizing the deviation from the experimental data) and applied in order to take into account the influence of the phenomena that are not directly modelled and the radiative contribution heat transfer from the flue gases.

$$h^i_{c,F,inner} = \frac{0.023 \cdot k_{g,F}}{2 \cdot R_{Flame}} Re_i^{0.8} Pr_i^{0.4} \tag{5}$$

Hottel and Sarofim [44] correlation, is instead employed to model the radiative heat transfer acting along the radial axis between the furnace wall (assumed to be Lambertian gray surfaces) and the the flame (which is treated as gray surface). Therefore, the global isotropic

emissivity is considered to be equivalent to the total absorptivity. The radiative heat flux formulation is correspondingly reported in Eq. 6.

$$\dot{q}^{i}_{rad,F} = \frac{2\pi R_{F,internal} L_F}{N_F} \sigma \frac{\varepsilon_{wall,F}\varepsilon_{g,F}}{\varepsilon_{g,F} + \varepsilon_{wall,F} - \varepsilon_{g,F}\varepsilon_{wall,F}} (T^{4,i}_{g,F} - T^{4}_{wall,F}) \tag{6}$$

Which can be further simplified resulting in Eq. 7.

$$\dot{q}^{i}_{rad,F} = \frac{2\pi R_{F,internal} L_F}{N_F} \sigma \frac{\varepsilon_{wall,F} + 1}{2} \varepsilon_{g,F} (T^{4,i}_{g,F} - T^{4}_{wall,F}) \tag{7}$$

Where the flame emissivity is dependant upon the fuel's origin. The natural gas flame global emissivity is equal to 0.21. It is also worth noticing that utilizing some fuel types can result in the generation of un-burned hydrocarbons and soot and the contribution of the latter components to the radiative heat transfer should be taken into account. Since the considered boiler is fed by natural gas, it has a negligible production of incandescent soot particles and the corresponding thermal radiative term is accordingly neglected.

The dynamic heat balance equation at the combustion chamber (represented by Eq. 8) is next utilized to model the heat transfer between the gases and the water in the shell side. In this equation, the dynamic thermal behavior of the walls should be taken into account (which is considered utilizing the the thermal capacity of the walls). The latter term is therefore affecting the heat flux transferred to water, which is driven by the convective and radiative heat transfer terms of the flue gas side.

$$m_{t,F} c_{P_{t,F}} \frac{d}{dt} T_{wall,F} = \sum_{i=1}^{N_F} \dot{q}^{i}_{rad,F} + \dot{q}^{i}_{conv,F} - \dot{q}_{water,F} \tag{8}$$

Where $\dot{q}_{water,F}$ is analytically expressed by Eq. 9 [43] .

$$\dot{q}_{water,F} = A_F U_{cond,conv} (T_{wall,F} - T_{water}) = \frac{2\pi R_F L_F}{\frac{R_F}{k_{t,F}} ln(\frac{1}{1-\frac{\bar{e}_F}{R_F}}) + \frac{1}{\bar{h}_{nb}}} (T_{wall,F} - T_{water}) \tag{9}$$

The proposed formulation is obtained while assuming isothermal walls and homogeneous distribution of water temperature inside the boiler's vessel. The heat flux term at the stagnation point is instead described by Eq. 10.

$$\dot{q}^{i}_{conv,F,bottom} = \pi R^{2}_{F,internal} h^{i}_{c,F} (T^{i}_{g,F} - T_{wall,F}) \tag{10}$$

2.2.3. Reverse flow gas side

The combustion process is no longer present in the reverse flow section, which leads to notably lower radiative heat transfer contribution of hot flue gases. Therefore, the heat balance (as reported in Eq. 11) is considered to model the annular shaped reverse flow stream.

$$\frac{d}{dt} (\rho_{g,H} V C_{v,g,F} T^{i}_{g,F}) = \dot{m}_g \bar{c}_{P,g,F} (T^{i-1}_{g,F} - T^{i}_{g,F}) - \dot{q}^{i}_{conv,F} + \dot{q}^{i}_{conv,F,inner} \tag{11}$$

It is noteworthy that, as was previously pointed out, although the radiative heat transfer contribution is not directly considered for the flue gas species, correction terms are included in Dittus-Boelter convective heat transfer equation.

2.2.4. Gas passes

Flue-gases, at intermediate temperature, exchange heat while passing through a set of horizontal tubes. Eq. 12 describes the mentioned phenomena while considering an even distribution of flue gas's volumetric flow (as previously motivated) between the set of (n) tubes among the existing ($j = 2, 3, 4, ..$) tube banks.

$$\frac{1}{n_{t,j}}\frac{d}{dt}(\rho_{g,j}V_j c_{V,g,j}T^i_{g,j}) = \frac{\dot{m}_g}{n_{t,j}}\overline{c}_{P,g}(T^{i-1}_{g,j} - T^i_{g,j}) - \dot{q}^i_{conv,j} \tag{12}$$

Heat transfer mechanism, occurring at each gas pass is described by a similar methodology including only the convective and conductive (through the tube walls) heat transfer terms. Therefore, the heat transfer rate through convection across the gas-pass walls and the rate of heat transfer to the water can be determined employing Eqs. 13 and 14.

$$m_{t,j}c_{P_{t,j}}\frac{d}{dt}T_{wall,j} = \sum_{i=1}^{N_j}\dot{q}^i_{conv,j} - \dot{q}_{water,j} \tag{13}$$

$$\dot{q}_{water,j} = A_j U_{cond,conv}(T_{wall,j} - T_{water}) = \frac{2\pi R_j L_j}{\frac{R_j}{k_{t,j}}ln(\frac{1}{1-\frac{\overline{e}_j}{R_j}}) + \frac{1}{\overline{h}_{nb}}}(T_{wall,j} - T_{water}) \tag{14}$$

2.2.5. Water-vapor side

Three different streams should be taken into account that cross the boundary of the considered vessel: the feed water flow, the extracted steam flow, and the periodic purge water stream. The latter one ($\dot{m}_p$) is the flow of water that is periodically extracted aiming at reducing the dissolved mass of salts due to the evaporation process and the further extraction of vapor. The inlet feed water flow ($\dot{m}_f$) introduced at given T_f conditions is controlled by a multi-stage centrifugal pump.

As demonstrated in Fig. 3, the boiler vessel is designed to facilitate the evaporation process through providing a considerable contact surface between the homogeneous liquid phase (lower side $-$) and the gaseous vapor phase (upper side $+$), represented by the separation surface. The water level is carefully controlled to assure that the tube banks (gas passes) are surrounded by water at any operating condition. The water-side heat exchange mechanism is described by the convective nucleate pool boiling that is induced by nucleation spots along the tubes microscopic roughness. Accordingly, convective nucleate boiling in an enclosed surface, through utilizing Cooper pool boiling correlation [45] (while considering the tubes' maximum nucleation radius to be $5\mu m$) is introduced to describe the corresponding heat transfer phenomenon, as described in Eq. 15.

$$h_{nb,j} = 12.96Pr^{0.12}[-0.4343 \cdot ln(Pr)]^{-0.55} \cdot \left(\frac{\dot{q}_{water}}{A_j}\right)^{0.67} \tag{15}$$

The latter correlation can be employed for the saturated pressure from 2 to 15 *bar* under the hypothesis of homogeneous distribution of the separate liquid and vapor phases

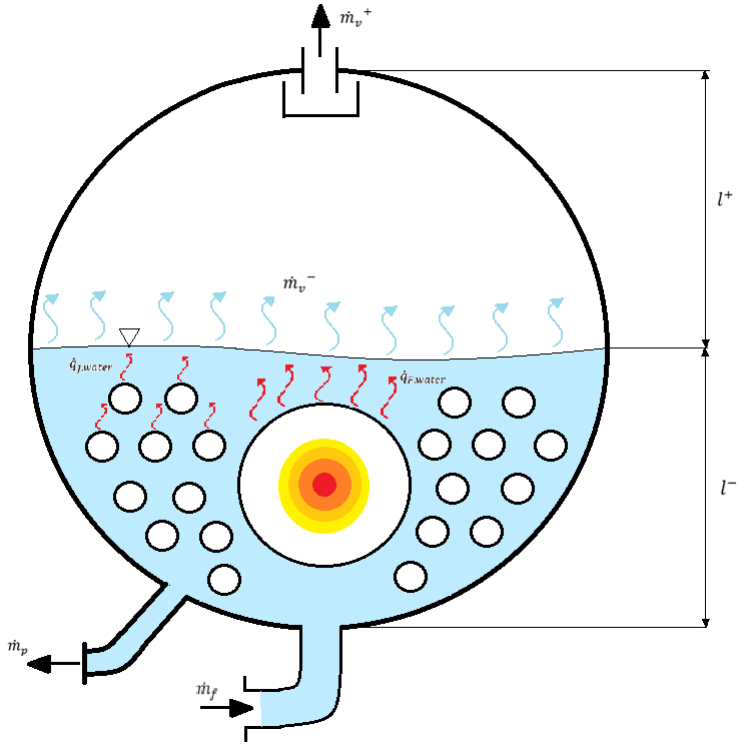

Figure 3: Schematic description of the evaporation process at liquid-vapor interface

at thermal equilibrium condition. The application of the mentioned nucleate pool boiling model throughout the external wall surfaces, results in considerably higher (compared to the flue-gas side convective heat transfer mechanism) convective heat transfer coefficient, which leads to limited temperature gradient between the tube's external temperature and the saturated surrounding water temperature. The mixing phenomena is therefore promoted by the mentioned effective nucleate pool boiling heat transfer mechanism. The description of the mentioned sub-sections (water and vapor sides) is provided below.

2.2.6. Vapor side/Upper zone (+)

Owning to the evaluation of the dynamic mass balance at the water-side (inside the boiler vessel), the dynamic thermal transients of the vapor quantity are much faster than those of the notably denser water portion (which is the main driver of the dynamic thermal phenomena at the water side); therefore, the dynamic energy balances is accordingly simplified. The thermal inertia effect of the saturated vapor mass has been neglected due to its negligible influence on the water/vapor side's heat balance. Therefore, the evaporated mass flow rate is equivalent to the one extracted through the steam extraction valve. From the proposed mass balance equation, the volume occupied by the vapor as a function of the water level is correspondingly reported in Eq. 16.

$$V^+ \simeq 2RLl^+ - \frac{4-\pi}{2}R^2L \tag{16}$$

The mentioned approximation, initially reported by Gutierrez Ortiz [31], reflects the assumption that the water level coincides with the average boiler's height, while the variation of vapor volume in time is expressed by Eq. 17.

$$\frac{dV^+}{dt} = \frac{dV^+}{dl^+} \cdot \frac{dl^+}{dt} \tag{17}$$

Thus, through combining the previous formulations, the (temporal) variation of the vapor volume can be determined employing Eq. 18.

$$\frac{dV^+}{dt} = 2R_{boiler}L_{boiler} \cdot \frac{dl^+}{dt} \tag{18}$$

2.2.7. Water-side/lower zone (-)

The unsteady mass balance of the water portion accounts for the three mass flow rates that cross the boundaries of the subsystem: feed water, purge, and the evaporation flow rate (as represented in Eq. 19).

$$\frac{d}{dt}(\rho^- V^-) \approx \rho^- V^- \frac{dV^-}{dt} = \dot{m}_f - \dot{m}_p - \dot{m}_v \tag{19}$$

Next, Taking into account the balance equation for the total volume of the liquid (which is considered to be incompressible), the variation in the volume of the liquid phase is equal to the variation in the volume of the vapour phase [31]. The steam extraction valve is driven by the pressure difference between the boiler shell and the downstream pressure, as expressed in Eq. 20.

$$\dot{m}_v^+ = K_{VS}C^s f_s(x)\sqrt{\rho^+(P^+ - P_{sum})} \tag{20}$$

Where the term K_{VS} is the valve flow coefficient, f_s represents the valve open factor while C^s is a conversion unit factor. The former mass balance Eq. 19 of the water-side is consequently arranged in order to include the previously introduced Eq. 20 resulting in Eq. 21:

$$-2RL\rho^- \frac{dl^+}{dt} = \dot{m}_f - \dot{m}_p - K_{VS}C^s f_s(x)\sqrt{\rho^+(P^+ - P_{sum})} \tag{21}$$

Finally, the energy balance with respect to the boiler's shell conditions is described in Eq. 22.

$$\frac{d}{dt}T_{water} \simeq \frac{1}{\rho V_{total}\bar{c}_V}[\dot{m}_f \bar{c}_{P,f}(T_f - T_{water}) - \dot{m}_v^+ \overline{\lambda} + \dot{q}_{F,water} + \sum_{j=2}^{3,4} \dot{q}_{j,water}] \tag{22}$$

Finally, the boiler first principle efficiency is determined as the ratio between the net thermal energy required to reach the desired extraction point (from the feed-water inlet conditions) and the thermal energy released due to the combustion process. Furthermore, the first principal thermal boiler efficiency (which inherently considers the purged mass flow rate) can be determined using Eq. 23.

$$\eta_{boiler,1^{st}} = \frac{\sum_{t=0}^{t=T_s} m_{v,t}^+ h_{v,t}^+ - m_{f,t}h_{f,t}}{\sum_{t=0}^{t=T_s} m_{fuel,t}LHV_{NG}} = \frac{\sum_{t=0}^{t=T_s} m_{v,t}^+ (h_{v,t}^+ - h_{f,t}) - m_{p,t}h_{f,t}}{\sum_{t=0}^{t=T_s} m_{fuel,t}LHV_{NG}} \tag{23}$$

It is noteworthy that the energy terms represent the corresponding net values determined from the beginning of the simulation (t =0) till $t = T_s$.

3. Description of the proposed control strategy

The controller employed in the considered boiler, modifies the fuel flow rate aiming at keeping the steam pressure close to the desired set-point at any instant. In this type of boilers, Proportional-Integral-Derivative (PID) controller is traditionally utilized, the operation principle of which is based on a control function [46]. The latter function describes the bias between the closed-loop feedback and the desired set-point, utilizing a set of tuned constant parameters. These parameters are commonly tuned through conducting an experimental procedure, while operating at nominal thermal power generation. PID controllers are robust and do not embody a system state, which simplifies their deployment in industrial devices. However, these controllers are sub-optimal and show limited performance while being employed for controlling non-linear systems like fire-tube boilers [47].

Motivated by the latter shortcoming, a novel dynamic PID controller is introduced aiming at reducing the observed transients, while the boiler is operating at non-nominal pressure set-points. Dynamic coefficients are thus introduced in the controller's state function, which are dependant upon the current feedback variable. The proposed control equation [48], in continuous terms, is described by Eq. 24:

$$u(t) = P_{PV}(t)[SP(t) - PV(t)] + I_{PV}(t)\int_0^t SP(\tau) - PV(\tau)d\tau + D_{PV}(t)\frac{d(SP(t) - PV(t))}{dt} \tag{24}$$

Where the dependency of the variable coefficients P, I, and D, on the process variable, is obtained through conducting a set of simulations. In these simulations, the validated physical model is utilized and the tests on three different process variables are conducted. These tests are carried out while operating at different pressure levels (including $2, 6$ and $10\ barg$). As can be observed in Table 2, the variations in the latter coefficients, obtained while attempting to keep the response time homogeneous in different tests, is considerable.

	$2\ barg$	$6\ barg$	$10\ barg$
P_{PV} coefficients	1132.53	299.62	253.66
I_{PV} coefficients	5.53	2.28	1.38
D_{PV} coefficients	16571.03	7044.09	4080.88

Table 2: Tuned pressure dependant coefficients utilized in the proposed dynamic PID controller

The proposed dynamic controller improves the controllability of the system in a wider range of operating conditions; which thus mitigates the undesired transients at lower pressure levels (compared to the nominal value).

4. Model validation

As was previously mentioned, the employed dynamic model was developed and validated in a previous work of the authors [39]. The corresponding results are briefly reported here in order to provide the reader with complete information. The experimental validation

procedure was performed utilizing two different boiler models manufactured by the industrial partner (ICI Caldaie S.p.A.) [39]. In order to conduct the measurement procedure, sensors were installed at the key locations of the boiler. Accordingly, temperature probes measure the average bulk flow temperature at the air premixing stage, the reverse flow chamber, the flue gas stack, and the feed water section. Pressure is instead measured at the water-side inside the boiler vessel and downstream of the steam extraction valve. In addition, volumetric flow rate measurement units were installed at the natural gas supply section and at the saturated vapor's supply side. The ambient conditions and the range of boiler's operating conditions that were considered in the validation procedure are reported in Table 3. It is worth mentioning that the stack's oxygen concentration was monitored and the same value was considered in the model in order to assure that a coherent combustion quality is taken into account [39].

Parameters	Values
Feed water temperature [° C]	70
Ambient temperature [° C]	30
Ambient pressure [bar]	1.01325
Ambient relative humidity [%]	30
Maximum hourly fuel mass flow rate [kg/h]	100
Flue gas oxygen volumetric concentration [$\%v$]	3.5
Maximum hourly feed-water mass flow rate [kg/h]	3000
Purge hourly mass flow rate [kg/h]	72

Table 3: Ambient conditions and the range of boiler's operating conditions that were considered in the model validation procedure (conducted in [39])

The validation tests consisted of a set of steady-state and dynamic behaviour assessments, in which the reverse flow chamber temperature and the boiler vessel pressure were considered as parameters to be validated. A calibration procedure, aimed at simulating the radiative heat transfer contribution at gas passes, was first conducted. Employing a portion of the experimentally obtained dataset, the corresponding calibration coefficients were accordingly tuned and applied. Next, the remaining set of data was employed in order to verify the agreement between the experimental data and the values estimated by the model (while simulating the boiler's behaviour for a range of operating conditions) [39].

Sub-section 4.1 presents the results of the validation procedure for the boiler model that is utilized in the present study (performed and presented in [39]), the specifications of which are reported in Table 4.

4.1. Validation results

In the steady-state validation step, the steam extraction valve's position was controlled in order to impose step-wise steam flow rates, while maintaining the boiler vessel pressure at 10 $barg$. Fig. 4 represents the comparison between the measured reverse flow chamber temperature, while performing the mentioned procedure, and the values estimated by the model

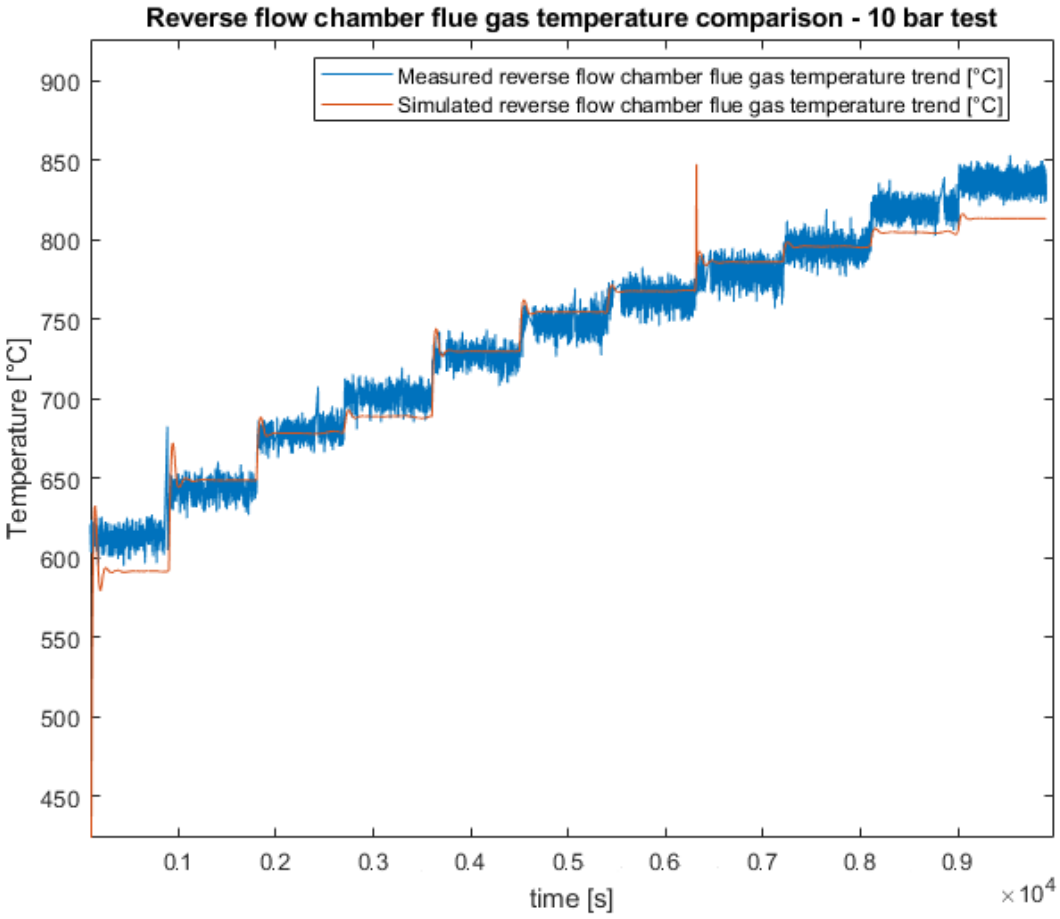

Figure 4: Comparison between the simulated values of reverse flow chamber temperature and the experimental data, while supplying different steam flow rates (from the results of the validation procedure performed and presented in [39])

[39]. The obtained results demonstrate a general agreement between the values estimated by the model and the experimental data. The largest difference between the measured average steady-state data and the corresponding simulated value was determined to be 2.8% [39].

In the next step, a procedure focused on verifying the validity of the developed model in simulating the dynamic behaviour of the boiler (while addressing transient thermal loads) was conducted. In this procedure. the boiler's pressure while applying instantaneous changes on the position of the steam extraction valve, was measured. The obtained results, presented in Fig. 5, demonstrated the consistency between the measured data and the simulation results (the highest bias was 1.2 %) [39].

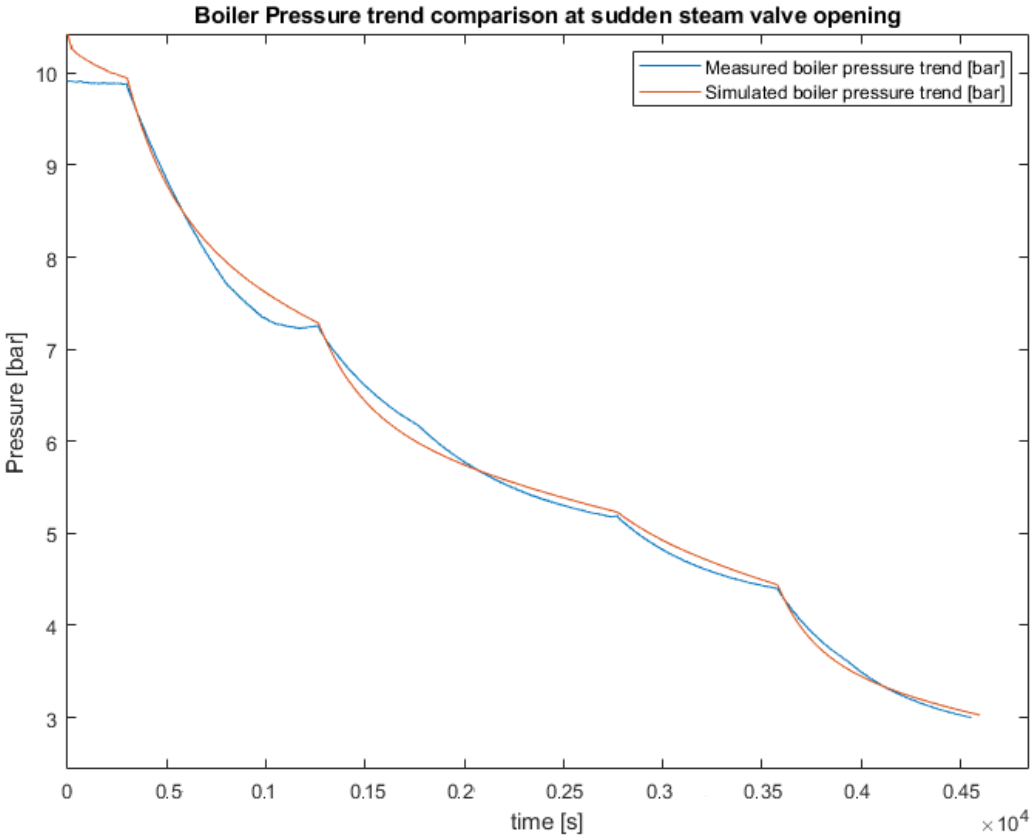

Figure 5: Comparison between the simulated transient boiler pressure profiles with the experimentally measured data, while undergoing an instantaneous steam extraction valve opening (from the results of the validation procedure performed and presented in [39])

5. Results and discussions

As was previously pointed out, a simulation is first performed aiming at assessing the controllability of the fire-tube boiler, while addressing a variable steam demand profile employing a multi-setpoint control strategy. In this simulation, the improvement obtained in the boiler's pressure tracking capability through utilizing the proposed dynamic PID controller, compared to a conventional PID controller, is determined. In the next step, the required fuel quantity utilizing the proposed multi-setpoint strategy (employing the mentioned dynamic PID controller) is compared with the one needed using the currently employed constant-setpoint approach.

Key characteristics and geometric configuration of the boiler considered in the simulation (the validation results of which were presented in the previous section) are reported in Table 4. The steam demand profile of an Italian cheese factory, which is considered as the case study (end-user) in the present work, is depicted in Fig. 6 (left). Fig. 6 (right) instead represents the daily variations in the desired pressure level (between 2 to 10 $barg$) of the

considered end-user, that is due to the utilization of different units throughout the day that require various levels of steam pressure. This figure also demonstrates the constant pressure setpoint of the boiler (10 $barg$) that is currently imposed by the considered end-user (while employing pressure reducers in the intervals that a lower pressure is needed).

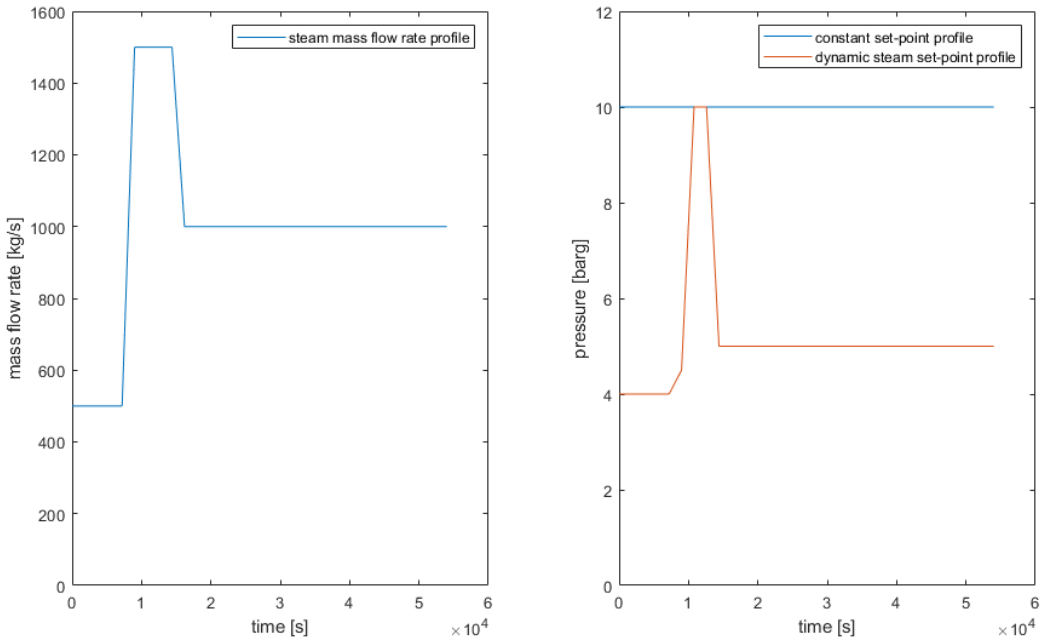

Figure 6: The daily variations in the steam mass flow rate and the desired pressure level of the considered end-user

The considered environmental conditions and the range of operating conditions of the boiler are the same as the ones employed in the validation procedure (reported in Table 3) with the difference that the feed water temperature is considered to be 60 ° C, the ambient relative humidity to be 50%, the maximum fuel mass flow rate to be 150 kg/h, and the purge mass flow rate to be 70 kg/h (with a cyclical time of 30 min).

Boiler net vessel volume $[m^3]$	Mass of metal parts $[kg]$	Heat transfer surface $[m^2]$	Net water volume/Heat transfer surface ratio $[m]$
2.28	893.05	23.78	0.0622

Table 4: Geometrical characteristics of the considered boiler

5.1. Controllability assessment and comparative analysis of controllers

The capability of the boiler in providing the desired pressure at any interval is important considering the possibility of having pressure sensitive downstream processes. Furthermore,

excessive fluctuation in the pressure can induce undesired cyclical stresses on the plant's components. Thus, the pressure controllability while implementing the proposed strategy should be first assessed. As was explained in Section 3, a dynamic PID controller is proposed in the present study in order to improve the pressure tracking capability of the boiler while imposing different setpoints. Accordingly, the improvement obtained in the pressure tracking capability of the boiler through employing the proposed dynamic PID controller, compared to the one achieved using a traditional PID controller, is calculated. The steam pressure bias that determines the deviation of the boiler pressure from the instantaneous desired setpoint, as expressed in Eq. 25, is employed as a metric for assessing the pressure tracking capability.

$$e = \sum_{0}^{T_s} \frac{[p(t) - p_{setpoint}(t)]^2}{n_{T_s}} \tag{25}$$

The pressure profiles that are obtained utilizing the proposed dynamic PID controller and the traditional PID, while imposing the desired pressure levels (depicted in Fig. 6(right)) as variable setpoints, are determined. The comparison between the obtained steam pressure bias, reported in Table 5 demonstrates the advantage of utilizing the proposed dynamic PID controller.

	Steam pressure bias $[bar^2]$
Traditional PID	0.1573
Dynamic PID	0.1564

Table 5: Steam pressure bias obtained while employing the traditional PID and the proposed dynamic PID controller

It is worth mentioning that the attempt to rapidly increase the pressure (owing to the increment in the desired pressure) is limited by the upper bound of the mass flow rate range of the combustor. On the other hand, while attempting to reduce the pressure, the highest pressure reduction rate can be obtained through turning the combustor off thus removing any heat release term, while having any further reduction rate is not practically possible. Fig. 7 graphically represents the difference in the obtained pressure profile, while utilizing the two controllers, which confirms the advantage of employing the proposed dynamic PID controller. Accordingly, in the procedure dedicated to the estimation of fuel saving potential of implementing the multi-setpoint strategy, the proposed controller is utilized.

5.2. Estimation of the fuel saving potential of implementing multi-setpoint control strategy

In the present section, a comparative analysis is performed in order to determine the amount of fuel saving that can be obtained through implementing the described multi-setpoint control strategy. Accordingly, the fuel quantity consumed by the boiler while imposing a constant pressure setpoint of 10 $barg$ is calculated and is compared with the determined amount of consumed fuel while utilizing a multi-setpoint strategy (considering the desired pressure levels indicated in Fig. 6(right)). Fig. 8 illustrates the intervals with

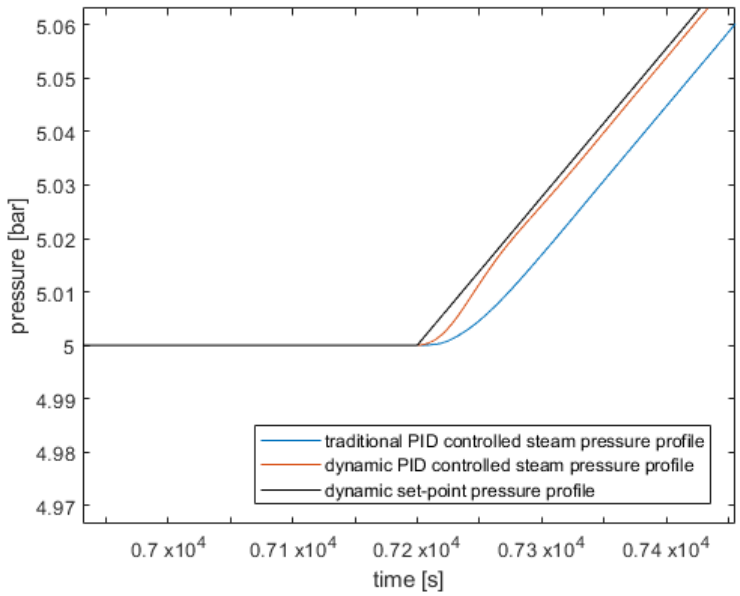

Figure 7: The comparison between the steam pressure profiles obtained using the traditional PID controller and the proposed controller

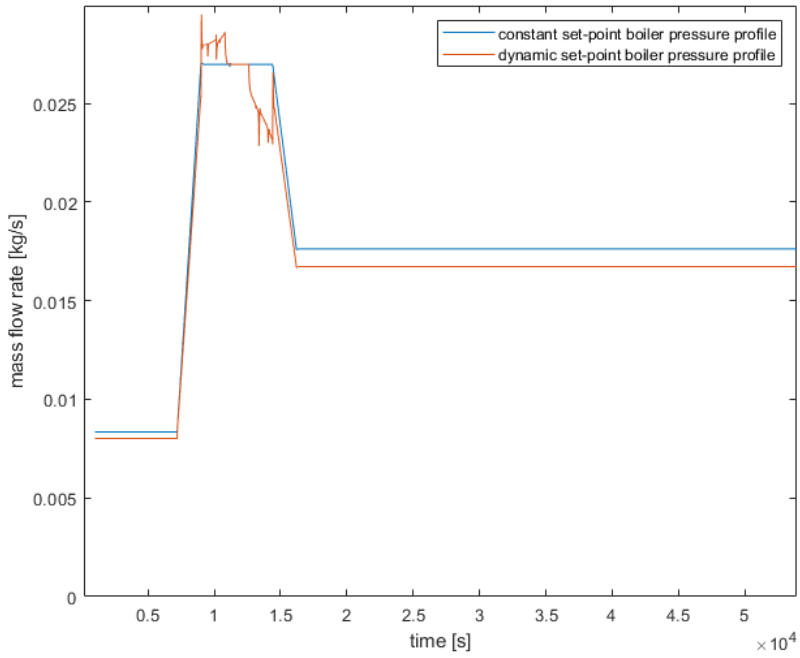

Figure 8: Comparison between the required hourly fuel flow rate, while employing the constant-setpoint and multi-setpoint strategies

fuel saving potential through implementing the multi-setpoint strategy, in which the reduction in fuel flow rate is a function of the corresponding reduction in the boiler's pressure. It is also worth noting that the estimated fuel hourly mass flow rate trend in the interval between $0.75 \cdot 10^4[s]$ and $1.5 \cdot 10^4[s]$ while employing the multi-setpoint strategy (as shown in Fig. 8) notably deviates from the one determined using the single-setpoint control strategy. The latter observation is the results of the variations in the imposed pressure setpoint (following the dynamic pressure set-point strategy) and the required variable steam flow rate, while the dynamic PID controller constantly attempts to minimize the discrepancy between the actual pressure of the boiler (inside the vessel) and corresponding setpoint through acting on the provided fuel mass flow rate, which in turn leads to fluctuations in the latter parameter.

While considering 300 working days (indicated by the considered end-user), the total yearly consumed fuel mass and the resulting cost (determined as the product of the yearly consumed fuel mass, the natural gas density, and the natural gas unitary price as reported in Table 6), for each control strategy, are determined (unitary gas price, from the Italian natural gas market, is assumed to be equal to 0.34 €/Sm^3).

Parameters	Values
Natural gas volumetric price [€/Sm^3]	0.34
Natural gas density [kg/Sm^3]	0.717

Table 6: Natural gas volumetric price and density that is employed in the economic analysis

The obtained results, reported in Table 7, demonstrate a notable fuel saving that can be achieved through utilizing the proposed multi-setpoint strategy, which (considering 20 years of operation) will lead to a net cost savings of around 120,000 €, while it does not require any hardware investment and only needs updating the control scheme, imposing different setpoints and PID tuning parameters for different intervals.

Employed control strategy	Yearly consumed fuel's mass [kg]	Yearly fuel cost [€]
Constant-setpoint	935.9	133,143
Multi-setpoint	893.7	127,143

Table 7: Consumed fuel mass and the resulting yearly fuel cost, while employing constant-setpoint and multi-setpoint strategies

6. Conclusions

The present study was conducted aiming at estimating the fuel saving potential of implementing a multi-setpoint control strategy in a fire-tube boiler (equipped with SPRF-type combustor), while addressing a variable steam demand profile. A detailed dynamic model of the boiler, validated using experimental data in a previous study by the authors, was accordingly employed. As the case study, the daily steam demand profile of an Italian cheese factory, including the corresponding flow rate and required pressure, were considered.

In order to improve the controllability of the boiler while implementing the mentioned strategy, a dynamic PID controller (tuned at different operating conditions) was first proposed. The resulting improvement in the boiler's pressure tracking capability, compared to the one obtained using traditional PID controller, was demonstrated. Next, while employing the proposed controller, the multi-setpoint control strategy was implemented and the resulting yearly fuel consumption of the boiler was determined and compared with the consumption of the unit utilizing the currently employed constant-setpoint strategy. It was demonstrated that employing the proposed methodology results in a significant fuel saving, which can lead to a net cost saving of around 120,000 € in 20 years of operation for the considered case study. The mentioned notable saving is obtained despite the fact that implementing the strategy does not require any additional hardware investment and will only necessitate imposing various pressure setpoints and PID parameters for different intervals. Since in the food and beverage industry, specifically in Italy, fire-tube boilers often feed multiple devices and the requested pressure level (throughout the day) is commonly highly variable, the methodology proposed in the present paper can be applied to several similar cases resulting in a significant fuel saving without requiring a notable investment.

7. Acknowledgments

The authors would like to thank ICI Caldaie S.p.A. for providing technical and financial support for this project. The corresponding activities, managed by ICI Caldaie, have been conducted in the context of the Ecovapor project (funded by the European union's Horizon 2020 research and innovation program under grant agreement no 730790).

References

[1] K. Harris, Model Boilers and Boilermaking, MAP technical publication, Model and Allied Publications, 1974.

[2] M. K. Bobba, P. Gopalakrishnan, J. Seitzman, B. Zinn, Characteristics of combustion processes in a stagnation point reverse flow combustor, in: ASME Turbo Expo 2006: Power for Land, Sea, and Air, American Society of Mechanical Engineers Digital Collection, 2006, pp. 867–875.

[3] S. Undapalli, S. Srinivasan, S. Menon, Les of premixed and non-premixed combustion in a stagnation point reverse flow combustor, Proceedings of the Combustion Institute 32 (1) (2009) 1537–1544.

[4] M. ÖZGÜNOĞLU, A. G. GÜNGÖR, Large eddy simulation of a stagnation point reverse flow combustor, Journal of Aeronautics and Space Technologies 12 (1) (2019) 75–85.

[5] V. Parisi, Large eddy simulation of a stagnation point reverse flow combustor, Ph.D. thesis, Georgia Institute of Technology (2006).

[6] v. P. Colonna, H. Van Putten, Dynamic modeling of steam power cycles.: Part i—modeling paradigm and validation, Applied Thermal Engineering 27 (2-3) (2007) 467–480.

[7] F. De Mello, Boiler models for system dynamic performance studies, IEEE Transactions on Power systems 6 (1) (1991) 66–74.

[8] L. Sun, D. Li, K. Y. Lee, Y. Xue, Control-oriented modeling and analysis of direct energy balance in coal-fired boiler-turbine unit, Control Engineering Practice 55 (2016) 38–55.

[9] E. Adam, J. Marchetti, Dynamic simulation of large boilers with natural recirculation, Computers & chemical engineering 23 (8) (1999) 1031–1040.

[10] K. J. Åström, R. D. Bell, Drum-boiler dynamics, Automatica 36 (3) (2000) 363–378.

[11] H. Kim, S. Choi, A model on water level dynamics in natural circulation drum-type boilers, International Communications in Heat and Mass Transfer 32 (6) (2005) 786–796.
[12] J. M. Blanco, L. Vazquez, F. Peña, Investigation on a new methodology for thermal power plant assessment through live diagnosis monitoring of selected process parameters; application to a case study, Energy 42 (1) (2012) 170–180.
[13] S. Chandrasekharan, R. C. Panda, B. Natrajan Swaminathan, Dynamic analysis of the boiler drum of a coal-fired thermal power plant, Simulation 93 (11) (2017) 995–1010.
[14] Y. Zhou, D. Wang, An improved coordinated control technology for coal-fired boiler-turbine plant based on flexible steam extraction system, Applied Thermal Engineering 125 (2017) 1047–1060.
[15] P. Sunil, J. Barve, P. Nataraj, Mathematical modeling, simulation and validation of a boiler drum: Some investigations, Energy 126 (2017) 312–325.
[16] S. Kim, S. Choi, Dynamic simulation of the water-steam system in once-through boilers-sub-critical power boiler case, Transactions of the Korean Society of Mechanical Engineers B 41 (5) (2017) 353–363.
[17] A. El-Guindy, S. Rünzi, K. Michels, Optimizing drum-boiler water level control performance: A practical approach, in: 2014 IEEE Conference on Control Applications (CCA), IEEE, 2014, pp. 1675–1680.
[18] E. Oko, M. Wang, J. Zhang, Neural network approach for predicting drum pressure and level in coal-fired subcritical power plant, Fuel 151 (2015) 139–145.
[19] H. Zhao, J. Shen, Y. Li, J. Bentsman, Coal-fired utility boiler modelling for advanced economical low-nox combustion controller design, Control Engineering Practice 58 (2017) 127–141.
[20] F. Rinaldi, B. Najafi, Temperature measurement in wte boilers using suction pyrometers, Sensors 13 (11) (2013) 15633–15655.
[21] A. Abene, A. Rahmani, R. G. Seddiki, A. Moroncini, R. Guillaume, Heat transfer study in 3-pass fire-tube boiler during a cold start-up, Software Engineering 5 (4) (2018) 57.
[22] K. Sørensen, C. M. Karstensen, T. Condra, N. Houbak, Modelling and simulating fire tube boiler performance, in: Proceedings of SIMS, 2003, pp. 9–12.
[23] B. Najafi, A. H. Mamaghani, F. Rinaldi, A. Casalegno, Fuel partialization and power/heat shifting strategies applied to a 30 kwel high temperature pem fuel cell based residential micro cogeneration plant, International Journal of Hydrogen Energy 40 (41) (2015) 14224–14234.
[24] B. Najafi, S. De Antonellis, M. Intini, M. Zago, F. Rinaldi, A. Casalegno, A tri-generation system based on polymer electrolyte fuel cell and desiccant wheel–part a: Fuel cell system modelling and partial load analysis, Energy Conversion and Management 106 (2015) 1450–1459.
[25] M. Tognoli, B. Najafi, F. Rinaldi, Dynamic modelling and optimal sizing of industrial fire-tube boilers for various demand profiles, Applied Thermal Engineering 132 (2018) 341–351.
[26] P. J. Coelho, P. A. Novo, M. Carvalho, Modelling of a utility boiler using parallel computing, The Journal of Supercomputing 13 (2) (1999) 211–232.
[27] C. K. Westbrook, Y. Mizobuchi, T. J. Poinsot, P. J. Smith, J. Warnatz, Computational combustion, Proceedings of the Combustion Institute 30 (1) (2005) 125–157.
[28] A. Gómez, N. Fueyo, L. I. Diez, Modelling and simulation of fluid flow and heat transfer in the convective zone of a power-generation boiler, Applied thermal engineering 28 (5-6) (2008) 532–546.
[29] M. Pezo, V. D. Stevanovic, Z. Stevanovic, A two-dimensional model of the kettle reboiler shell side thermal-hydraulics, International journal of heat and mass transfer 49 (7-8) (2006) 1214–1224.
[30] B. Najafi, H. Najafi, M. Idalik, Computational fluid dynamics investigation and multi-objective optimization of an engine air-cooling system using genetic algorithm, Proceedings of the Institution of Mechanical Engineers, Part C: Journal of Mechanical Engineering Science 225 (6) (2011) 1389–1398.
[31] F. G. Ortiz, Modeling of fire-tube boilers, Applied Thermal Engineering 31 (16) (2011) 3463–3478.
[32] M. Barma, R. Saidur, S. Rahman, A. Allouhi, B. Akash, S. M. Sait, A review on boilers energy use, energy savings, and emissions reductions, Renewable and Sustainable Energy Reviews 79 (2017) 970–983.
[33] R. Saidur, J. U. Ahamed, H. H. Masjuki, Energy, exergy and economic analysis of industrial boilers, Energy policy 38 (5) (2010) 2188–2197.
[34] J. Bujak, Mathematical modelling of a steam boiler room to research thermal efficiency, Energy 33 (12)

(2008) 1779–1787.
[35] L. Chao, L. Ke, W. Yongzhen, M. Zhitong, G. Yulie, The effect analysis of thermal efficiency and optimal design for boiler system, Energy Procedia 105 (2017) 3045–3050.
[36] G. Hahn, Boiler efficiency vs. steam quality- the challenge of creating quality steam using existing boiler efficiencies (01 1998).
[37] S. Chandrasekharan, R. C. Panda, B. N. Swaminathan, A. Panda, Operational control of an integrated drum boiler of a coal fired thermal power plant, Energy 159 (2018) 977–987. doi:https://doi.org/10.1016/j.energy.2018.06.157.
URL https://www.sciencedirect.com/science/article/pii/S0360544218312222
[38] S. Spinelli, M. Farina, A. Ballarino, An optimal control of start-up for nonlinear fire-tube boilers with thermal stress constraints, in: 2019 18th European Control Conference (ECC), 2019, pp. 2362–2367. doi:10.23919/ECC.2019.8796156.
[39] M. Tognoli, B. Najafi, R. Marchesi, F. Rinaldi, Dynamic modelling, experimental validation, and thermo-economic analysis of industrial fire-tube boilers with stagnation point reverse flow combustor, Applied Thermal Engineering 149 (2019) 1394–1407.
[40] W. Beyne, D. Daenens, B. Ameel, M. Van Belleghem, S. Lecompte, M. De Paepe, Steady state modeling of a fire tube boiler, in: 13th International Conference on Heat Transfer, Fluid Mechanics and Thermodynamics, 2017.
[41] M. Flynn, M. O'Malley, A drum boiler model for long term power system dynamic simulation, IEEE Transactions on Power Systems 14 (1) (1999) 209–217.
[42] G. F. Hewitt, J. Barbosa, Heat exchanger design handbook, Vol. 98, Begell house New York, 2008.
[43] Y. Cengel, T. M. Heat, A practical approach, Mc-Graw Hill Education, Columbus, GA, USA, 2003.
[44] H. Hottel, A. Sarofim, Radiative transfer,(1967), New York 20–24.
[45] M. Cooper, Heat flow rates in saturated nucleate pool boiling-a wide-ranging examination using reduced properties, in: Advances in heat transfer, Vol. 16, Elsevier, 1984, pp. 157–239.
[46] M. Araki, Control systems, robotics and automation—vol ii—pid control, Kyoto University, Japan (2010).
[47] G. Pellegrinetti, J. Bentsman, Nonlinear control oriented boiler modeling-a benchmark problem for controller design, IEEE transactions on control systems technology 4 (1) (1996) 57–64.
[48] B. G. Lipták, Instrument engineers' handbook, volume two: Process control and optimization, Vol. 2, CRC press, 2018.